

PM_{2.5} as a major predictor of COVID-19 basic reproduction number in the USA

Ognjen Milicevic¹, Igor Salom², Marko Tumbas³, Andjela Rodic³, Sofija Markovic³, Dusan Zigic², Magdalena Djordjevic², Marko Djordjevic^{3,*}

¹Department for Medical Statistics and Informatics, School of Medicine, University of Belgrade, Serbia

²Institute of Physics Belgrade, National Institute of the Republic of Serbia, University of Belgrade, Serbia

³Quantitative Biology Group, Institute of Physiology and Biochemistry, Faculty of Biology, University of Belgrade, Serbia

* Correspondence:

Marko Djordjevic, e-mail: dmarko@bio.bg.ac.rs

Keywords: COVID-19 pollution dependence, outdoor air pollutants, basic reproduction number, principal component analysis, machine learning

Abstract

Many studies have proposed a relationship between COVID-19 transmissibility and ambient pollution levels. However, a major limitation in establishing such associations is to adequately account for complex disease dynamics, influenced by e.g. significant differences in control measures and testing policies. Another difficulty is appropriately controlling the effects of other potentially important factors, due to both their mutual correlations and a limited dataset. To overcome these difficulties, we will here use the basic reproduction number (R_0) that we estimate for USA states using non-linear dynamics methods. To account for a large number of predictors (many of which are mutually strongly correlated), combined with a limited dataset, we employ machine-learning methods. Specifically, to reduce dimensionality without complicating the variable interpretation, we employ Principal Component Analysis on subsets of mutually related (and correlated) predictors. Methods that allow feature (predictor) selection, and ranking their importance, are then used, including both linear regressions with regularization and feature selection (Lasso and Elastic Net) and non-parametric methods based on ensembles of weak-learners (Random Forest and Gradient Boost). Through these substantially different approaches, we robustly obtain that PM_{2.5} levels are the main predictor of R_0 in USA states, with corrections from factors such as other pollutants, prosperity measures, population density, chronic disease levels, and possibly racial composition. As a rough magnitude estimate, we obtain that a relative change in R_0 , with variations in pollution levels observed in the USA, is typically ~30%, going up to 70%, which further underscores the importance of pollution in COVID-19 transmissibility.

1 Introduction

Many studies have provided evidence or strong arguments for the importance of pollution (primarily $PM_{2.5}$ and to a lesser degree PM_{10} and NO_2) in COVID-19 transmissibility: *i)* Droplets with virus particles may bind to Particulate Matter (PM), which may promote the diffusion of virus droplets in the air (Chen et al., 2010; Comunian et al., 2020; Contini and Costabile, 2020). *ii)* Once the virus droplet bound to PM reaches a susceptible individual, it can penetrate deeper in alveolar and tracheobronchial regions (Qu et al., 2020). *iii)* Pollution has a general effect on weakening the immune system making the organism more susceptible to infection (Domingo and Rovira, 2020; Paital and Agrawal, 2020; Qu et al., 2020). *iv)* It promotes overexpression of ACE-2 receptors, which allows SARS-CoV-2 binding and entry into cells (Comunian et al., 2020; Paital and Agrawal, 2020; Sagawa et al., 2021).

While these arguments are compelling, and several studies pointed to correlations between pollutant levels and increased severity of COVID-19 progression (De Angelis et al., 2021; Lorenzo et al., 2021; Tello-Leal and Macías-Hernández, 2020; Yao et al., 2021; Zhu et al., 2020), there are also prominent methodological difficulties in establishing this link. Specifically, comparing case counts (Adhikari and Yin, 2020; Suhaimi et al., 2020) in different geographical regions may be influenced by significant differences in the epidemic onsets, applied control measures (social distancing and similar), and testing methodologies (most significantly the number of performed tests). Consequently, adequately controlling the infection dynamics, rather than relying on absolute case counts, is crucial. Secondly, confounding factors, which have to be used jointly with pollution in assessing transmissibility, such as social-demographic, medical, and meteorological variables can be mutually highly correlated (Salom et al., 2021). Such high correlations realistically present a problem for any statistical inference method, though modern machine-learning approaches can partially account for this difficulty (Gupta and Gharehgozli, 2020). Also, to obtain robust predictions that are not an artifact of the applied methodology and the underlying assumptions, it is crucial to perform analysis by several independent methods.

We will accordingly employ the following approach: *i)* We consider USA states as this dataset has sufficient variability in the relevant variables to extract reasonable conclusions while heterogeneities in sociodemographic and weather parameters are not too large to overshadow the dependence on pollution. *ii)* As a measure of transmissibility, we use the basic reproduction number (R_0), which is insensitive to specific testing policies and estimates SARS-CoV-2 transmissibility in the absence of social distancing and in a completely susceptible (non-resistant) population. To estimate R_0 for individual USA states, we will apply our previously developed methodology (Salom et al., 2021) based on observation of different dynamical regimes in COVID-19 infection counts during the disease outburst and disease dynamics model applied to one of these growth regimes (exponential). These R_0 estimates, instead of the disease counts (or other similar measures), will be used as a dependent (response) variable in further analysis. As independent (input) variables, we will assemble a large set of available sociodemographic, medical, and weather variables. Importantly, to assess the pollution levels in detail, we will assemble the data for ten different pollutants, with the levels determined in the time windows relevant for the analyzed exponential growth regimes. The weather parameters will be assembled in the same dynamically relevant manner. This will result in a large number of predictors, many of which are grouped in sets of similar and mutually often highly correlated variables. Additionally, the number of assembled variables will exceed the total sample size, so reducing the number of predictors to a smaller and less correlated set will become a priority. We will achieve this through data preprocessing (feature engineering), which includes variable transformations, removing all outliers, and grouping variables in mutually related and correlated subsets (e.g., measures of similarity, population age, prosperity, chronic disease). Principal Component Analysis (PCA) will be

applied on these subsets, resulting in dimensionality reduction (reducing the number of predictors) and smaller correlations within these reduced predictor sets. Finally, established machine learning approaches will be used with the goals to *i*) select important variables and rank their relative importance in explaining R_0 , *ii*) obtain an estimate of expected changes in R_0 based on observed variability in pollution levels. While this will be a rough estimate, due to the inability to assemble all relevant factors in determining R_0 , it will provide a quantitative assessment for the importance of pollution in SARS-CoV-2 transmissibility.

2 Methods

2.1 R_0 extraction

Basic reproduction number (R_0) is a measure of SARS-CoV-2 transmissibility in a fully susceptible population and in the absence of intervention measures (social distancing, quarantine). For extraction of R_0 , we used our previously published methodology, in particular analysis of widespread infection growth regimes (Magdalena Djordjevic et al., 2021) and extraction of R_0 from the exponential growth phase that we previously applied on a worldwide level (Salom et al., 2021). We below for completeness summarize this methodology.

To describe the SARS-CoV-2 transmission in a population, we constructed an adapted version of an SEIR compartmental model (Maier and Brockmann, 2020; Maslov and Goldenfeld, 2020; Perkins and España, 2020; Tian et al., 2020; Weitz et al., 2020), which takes into account all the relevant features of this process, while being simple enough to be used for R_0 estimation in a wide range of populations (Magdalena Djordjevic et al., 2021; Salom et al., 2021). In the early stages of epidemics and before social distancing measures are introduced, the flow between the model compartments leads to the changes of the compartment member abundances S (susceptible), E (exposed), I (infected), R (recovered), and D (cumulative detected cases) which are described by the following system of ordinary differential equations:

$$\frac{dS}{dt} = -\frac{\beta SI}{N} \quad (1.1.)$$

$$\frac{dE}{dt} = \frac{\beta SI}{N} - \sigma E \quad (1.2.)$$

$$\frac{dI}{dt} = \sigma E - \gamma I \quad (1.3.)$$

$$\frac{dR}{dt} = \gamma I \quad (1.4.)$$

$$\frac{dD}{dt} = \varepsilon \delta I \quad (1.5.)$$

where N is the population size. Parameters represent: β - the rate of virus transmission from an infected to the encountered susceptible individual, σ - the inverse of the average incubation period (~ 3 days), γ - the inverse of the average period of infectiousness, ε - the detection efficiency (as not every infected individual becomes detected), and δ - the detection rate.

We here apply the model to the relatively brief, initial epidemics period when government mitigation measures were still absent, the virus spreads according to its biological potential, the characteristics of the particular population, and the environment. Therefore, the parameter values are considered constant in this period. The standard measure of the virus transmissibility in these, uncontrolled conditions is the basic reproduction number, R_0 , defined as the average number of secondary infections caused by a primary infected individual in a fully susceptible population ($S/N \approx 1$), and in the absence of social distancing measures (also sometimes denoted as $R_{0,free}$) (Maier and Brockmann, 2020). At the start of an epidemic, $R_0 > 1$ and the number of the infected individuals grows exponentially. At this time

interval, the model can be linearized by invoking $S/N \approx 1$, becoming represented by only two linear differential equations (1.2) and (1.3). Solving for the eigenvalues of this system,

$$\lambda_{\pm} = \frac{-(\gamma + \sigma) \pm \sqrt{(\gamma - \sigma)^2 + 4\beta\sigma}}{2}, \quad (3.7.)$$

provides the solution of the form $I(t) = C_1 \cdot e^{\lambda_+ t} + C_2 \cdot e^{\lambda_- t}$, which can be approximated by

$$I(t) = I(0) \cdot e^{\lambda_+ t} \quad (3.8.)$$

where the term containing the negative eigenvalue, λ_- can be neglected (see (Salom et al., 2021)). With $R_0 = \beta/\gamma$ (Keeling and Rohani, 2011; Martcheva, 2015), the equation for the basic reproduction number,

$$R_0 = 1 + \frac{\lambda_+ \cdot (\gamma + \sigma) + \lambda_+^2}{\gamma \cdot \sigma}. \quad (3.9.)$$

can be obtained by expressing β from Eq. (3.7).

To estimate the R_0 values for 46 US states, we collect the detected case counts for each state from (Worldometer, 2020). The solution $D(t) = \varepsilon \cdot \delta \cdot I(0) \cdot (e^{\lambda_+ t} - 1)/\lambda_+$ of the Eq. (1.5) using the Eq. (3.8) models the dependence of the cumulative number of detected with time. Taking its logarithm,

$$\log(D(t)) = \log(\varepsilon \delta I(0)/\lambda_+) + \lambda_+ \cdot t, \quad (3.12.)$$

results in the equation of the straight line that can be fitted to the data on the semilogarithmic scale. Notably, the slope of that line is given by the positive eigenvalue of the system, λ_+ . Once that λ_+ is, thus, determined by fitting, the value of R_0 for a particular state can be calculated from Eq. (3.9).

2.1 Pollution data collection

Air quality information was obtained from the US environmental protection agency (EPA) Air Data service (US Environmental Protection Agency, 2020). We used aggregated daily data for pollutant gases (O_3 , NO_2 , SO_2 , CO), particulates ($PM_{2.5}$ and PM_{10}) and other available species (VOCs, NO_x , and HAPs). Aggregation was done over all the cities with available information (smaller in comparison to the cities used for weather data). The population was obtained from the US Census Bureau (U.S. Census Bureau, 2020). All the variable values are averaged for each city over the identified time period, and the state average is calculated as the average of all included state cities weighted by population.

2.4 Weather data collection

Weather parameters were downloaded in bulk using a custom Python script from the NASA POWER project service (NASA Langley Research Center, 2020). All the parameters were downloaded via the POWER API at the longitude and latitude coordinates matching the largest cities in each state that comprise above 10% of the state population. Variables include temperature at 2m and 10m, measures of humidity and precipitation (wet bulb temperature, relative humidity, total precipitation), and insolation indices. The maximum predicted UV index was downloaded from OpenUV (OpenUV, 2020). Geographical coordinates of the cities and populations of cities and states were adapted from Wikidata (Wikipedia, 2021a, 2021b).

1.3 Socio-demographic data collection

Demographic data was collected from several sources. The demographic composition of the U.S. population by gender, race, and percentage of the population under 18 and over 65 was taken from the Measure of America, a project of The Social Science Research Council website (Measure of America,

2018). Information about health insurance, GDP, life expectancy at birth, infant and child mortality was also taken from the Measure of America website. Medical parameters such as hypertension, cholesterol, cardiovascular disease, diabetes, cancer, obesity, inactivity, and chronic kidney and obstructive pulmonary disease were taken from the Americas Health Rankings website (America's Health Ranking, 2021) hosting Centers for Disease Control and Prevention (CDC) data (CDC, 2019). Percentages of the population that are actively smoking and consuming alcohol are taken from the same source as well. The percentage of the foreign population was taken from the Census Reporter website (U.S. Census Bureau, 2019). The subnational HDI was taken from the Global Data Lab website (2020) (Smits and Permanyer, 2019). Population density, urban population percentage, and median age were taken from the U.S. Census Bureau website (U.S. Census Bureau, Population Division, 2019).

2.5 Data processing

Analysis of data distributions and QQ plots reveals non-normal distributions in a majority of variables. To reduce the skewness of the data we applied a number of transforms with different strengths (square root, cubic root, or log), adjusted in sign to maintain the data ranking (Spearman correlation). The table with all applied transformations is provided below. Also, note that the entire dataset used in this analysis (variable values for all 46 states) is provided in Supplement Table 1. In addition to the transformations applied, the table below also links the variables to the dataset, by relating a variable shortcut (used in Supplemental files) with its full name and units.

Data	Name(units)	Transformation f(x)
T2M, T2M _{MAX} , T2M _{MIN} , T10M, T10M _{MAX} , T10M _{MIN} , TS, T2MWET	Temperatures (°C)	None
RH2M	Relative humidity at 2 meters (%)	$-\log(\max(x) - x)$
QV2M	Specific humidity at 2 meters (g/kg)	$\log(x)$
T2MDEW	Dew Point (°C)	None
PRECTOT	Precipitation (mm/day)	$x^{1/3}$
TQV	Total Column Precipitable Water (cm)	$\log(x)$
CLRSKY_SFC_SW_DWN	Clear Sky Insolation Incident on a Horizontal Surface (MJ/m ² /day)	$\log(x)$
ALLSKY_SFC_LW_DWN	Downward Thermal Infrared (Longwave) Radiative Flux (MJ/m ² /day)	$-(\max(x) - x)^{1/3}$
ALLSKY_SFC_SW_DWN	All Sky Insolation Incident on a Horizontal Surface (MJ/m ² /day)	$\log(x)$
OpenUV _{max}	UV radiation	$x^{1/3}$
WS2M	Wind speed at 2 meters	None
WS10M	Wind speed at 10 meters	None
Population over 65 (%)	Population over 65 (%)	None
Life Expectancy	Life Expectancy at Birth (years)	$-(\max(x) - x)^{1/2}$
Median age	Median age (years)	$-(\max(x) - x)^{1/2}$
Youth population	Population under 18 (%)	$\log(x)$
Population density	Population density (people/km ²)	$\log(x)$
BUAPC	Built Up Area Per Capita (km ² /people)	$\log(x)$

Pollution influence on COVID-19 R_0

Urban Population	Urban Population (%)	$-(\max(x) - x)^{1/2}$
HDI	Human development index (0-1) Average of education, health and standard of living. (Mean years of schooling of adults aged 25+, Expected years of schooling of children aged 6 + Life expectancy at birth + GNIpc) /3	$-(\max(x) - x)^{1/2}$
GDPpc	Gross domestic product per capita	$\log(x)$
Infant mortality rate	Infant Mortality Rate (per 1,000 live births)	$-\log(x)$
Child mortality	Child Mortality (age 1-4, per 1000 population)	$-\log(x)$
Alcohol consumption	Adults alcohol consumption binge drinking (%)	$\log(x)$
Foreign-born population	Foreign-born population (%)	$\log(x)$
Obesity	Obesity age 20 and older (%)	None
CVD deaths	Age 65+ Cardiovascular disease deaths per 100000 people	$\log(x)$
Hypertension	Adults with Hypertension (%)	$\log(x)$
High cholesterol	Population with high cholesterol (%)	None
Smoking	Population smoking (%)	None
Cardiovascular disease	Population with cardiovascular disease (%)	None
Diabetes	Population with diabetes (%)	$x^{1/3}$
Cancer	Population with cancer (%)	None
Chronic kidney disease	Population with chronic kidney disease (%)	$x^{1/2}$
Chronic obstructive pulmonary disease	Population with chronic obstructive pulmonary disease (%)	$\log(x)$
Multiple chronic conditions	Population with multiple chronic conditions (%)	None
Physical inactivity	Population physically inactive (%)	$x^{1/3}$
Male percent	Fraction of male in the population (%)	$\log(x)$
White percent	Fraction of white in the population (%)	$-\log(\max(x) - x)$
Black percent	Fraction of black in the population (%)	$x^{1/3}$
Native percent	Fraction of native in the population (%)	$\log(x)$
Asian percent	Fraction of Asian in the population (%)	$\log(x)$
Latino percent	Fraction of Latino in the population (%)	$\log(x)$
No health insurance children	No health insurance under 18 (%)	$x^{1/2}$
No health insurance adults	No health insurance 18-64 (%)	None
No health insurance all	No health insurance all population (%)	None

No insurance black	No health insurance black (%)	None
No insurance native	No health insurance native (%)	$x^{1/3}$
No insurance Asian	No health insurance Asian (%)	$x^{1/2}$
No insurance Latino	No health insurance Latino (%)	None
No insurance white	No health insurance white (%)	None
PM _{2.5}	PM _{2.5} concentration ($\mu\text{g}/\text{m}^3$)	None
PM ₁₀	PM ₁₀ concentration ($\mu\text{g}/\text{m}^3$)	$x^{1/2}$
CO	CO concentration (ppm, 10^{-6})	$x^{1/2}$
NO ₂	NO ₂ concentration (ppb, 10^{-9})	None
SO ₂	SO ₂ concentration (ppb)	$\log(x - \min(x))$
O ₃	O ₃ concentration (ppm)	None
VOC	Volatile organic compounds concentration (ppb Carbon)	$\log(x)$
Lead	Lead concentration ($\mu\text{g}/\text{m}^3$)	$\log(x)$
HAPs	Hazardous air pollutants concentration ($\mu\text{g}/\text{m}^3$)	$x^{1/2}$
NONOxNOy	Nitrous oxides concentration (ppb)	$x^{1/3}$
R ₀	Estimated basic reproduction number	$\log(x)$

Table 1. List of variables (with units) and the applied transformations. Variable shortcuts (first column) correspond to Supplement Table 1.

Individual data values that remained more than three median absolute deviations from the new median were substituted by the said median value.

2.6 Feature engineering and Principal Components Analysis

To reduce the number of variables, we divided them into groups by conceptual similarity and expected correlation and performed Principle Component Analysis (PCA) on each group. This also partially reduced data correlation (Joliffe, 2002). Variables are grouped according to two criteria: *i*) They represent similar quantities so that after PCA interpretation of the obtained PC remains unambiguous *ii*) That correlation between the variables in the same group are high, so that in this way after PCA the correlations in the predictor set are substantially reduced. Grouping of variables and their relation to PCA is provided in Table 2 below:

PC components	Variables
PC1 T	T2M, T2M _{MAX} , T2M _{MIN} , T10M, T10M _{MAX} , T10M _{MIN} , TS
PC1 humidity	QV2M, T2MDEW
PC1 percipitation	PRECTOT, TQV
PC1 radiation PC2 radiation	CLRSKY_SFC_SW_DWN, ALLSKY_SFC_SW_DWN, ALLSKY_SFC_LW_DWN
PC1 seasonality PC2 seasonality	PC1 T, PC1 humidity, PC1 precipitation, PC1 radiation, PC2 radiation, RH2M, UV
PC1 age	Population over 65, Youth population, Median age

PC2 age	
PC1 density PC2 density	1/BUCAP, Urban population, Population density
PC1 prosperity PC2 prosperity PC3 prosperity PC4 prosperity	Life expectancy, Infant mortality, GDP, HDI, Child mortality, Alcohol consumption, Foreign born population
PC1 disease PC2 disease PC3 disease PC4 disease	Obesity (% age 20 and older), Age 65+ CVD deaths, Adults with hypertension (%), Population with high cholesterol (%), Population smoking (%), Population with cardiovascular disease (%), Population with diabetes%, Population with cancer (%), Population chronic kidney disease (%), Population chronic obstructive pulmonary disease (%), Population multiple chronic conditions (%), Population physical inactivity (%),
PC1 ins. PC2 ins. PC3 ins.	No health insurance (% of _children_under_18), No health insurance (% of _adults_ages_18–64), No health insurance total population (%), No health insurance black (%), No health insurance native (%), No health insurance Asian (%), No health insurance Latino (%), No health insurance white (%),

Table 2. Grouping of variables and relation to PC.

Since different variables are expressed in different units and correspond to diverse scales, each variable in the dataset was standardized (the mean subtracted and divided by the standard deviation) before PCA. For each datasets, we retained as many PCs (starting from the most dominant one) as needed to (cumulatively) explain >85% of the data variance. It was inspected that PCs reasonably follow a normal distribution (as expected, based on the transformation of the original variables). Note that a number of variables did not enter any of the groups from Table 2, as they either have a distinct meaning from other variables (e.g. racial prevalence), or have a similar meaning but do not exhibit a high correlation with the related variables (e.g. relative humidity RH2M, which does not correlate well with the other two humidity measures, QV2M and T2MDEW). These variables enter further analysis independently, i.e. together with PCs obtained after PCA on grouped variables.

2.7 LASSO regression

To complement the feature selection already done through PCA, additional L1 regularization was done with Lasso (Tibshirani, 1996). All input variables were standardized. Hyperparameter λ controlling for the model complexity was optimized through grid search on an exponential scale from numerical zero (OLS regression) to the value yielding the intercept-only model. Mean Squared Error (MSE) on the cross-validation testing set (200 repeats, 80-20 split) was taken as the loss function, and we chose the λ_{1SE} as the simplest model still comparable to the optimal one (Krstajic et al., 2014). The final model was comprised of all the non-zero coefficients.

2.8 Elastic net regression

Elastic Net expands the Lasso regression with an L2 regularization and introduces a second hyperparameter α (Friedman et al., 2010; Hastie et al., 2008; Zou and Hastie, 2005). The same preprocessing was done for the input variables, after which the 2-dimensional grid-search with the same λ -scale as in Lasso, and the α linearly equidistant on the interval from 0 (Ridge regression) to 1 (Lasso regression) inclusive. Cross-validation was performed the same as for the Lasso regression, but each fold gave a distinct (α, λ) pair of hyperparameters. The final chosen value is the (α, λ) pair closest to the centroid of all the folds, and these hyperparameters were used to retrain the model on the whole dataset. Again, the final model was comprised of all the non-zero coefficients.

2.9 Random Forest and Gradient Boost

To avoid overfitting, variables were preselected so that they exhibit significant correlations with R_0 (with a liberal threshold of $P < 0.1$), by either Pearson, Kendall, or Spearman correlations. Cross-validation and hyperparameter selection for Gradient Boost and Random Forest (Breiman, 2001, 1996; Freund and Schapire, 1997; Friedman, 2001; Hastie et al., 2008) was done equivalently as for Lasso and Elastic net. For Gradient Boost, maximal number of splits, minimal leaf size, and learning rate were chosen through grid search, with the respective values: $\{1, 2, 3, 4, 5, 8, 16\}$; $\{1, 2, 3, 4, 5, 8, 16, 18\}$; $\{0.1, 0.25, 0.5, 0.75, 1\}$. For Random Forest, the grid values for maximal number of splits and minimal leaf size were, respectively: $\{6, 12, 18, 22, 24, 26, 30, 35\}$, $\{1, 2, \dots, 7\}$. The number of trained decision trees in the ensemble was also chosen to minimize Mean Square Error (MSE) on the testing set, for both methods. The obtained hyperparameters were used to retrain the models on the whole dataset, and predictor importance was estimated for both methods.

2.10 Model metrics

MSE for the testing data, averaged over all cross-validations, was used as a metric to compare the performance of different models. For easier interpretability, MSE values were scaled by those corresponding to the constant model (so that MSE of 1 corresponds to the constant model). To assess statistical significance with respect to the constant model, a t-test was applied to MSE values obtained through cross-validation.

3 Results

3.1 Extraction of R_0 and feature engineering

The $\log(D(t))$ in the exponential growth regime for a subset of selected USA states is shown in Fig. 1. The linear dependence confirms that the progression of the epidemic in this stage is almost perfectly exponential. Moreover, from Fig. 1, we see that this exponential growth in the cumulative number of confirmed cases is robustly observed for a wide range of USA states, while we previously also observed the same robust initial exponential growth for a wide range of world countries (Salom et al., 2021). This exponential growth happens in the early infection stage, when only a small fraction of the population is resistant, and before social distancing interventions take effect. Note that, even after introducing the measures, there is ~ 10 days delay in observing their effect in the confirmed case-counts curve, due to the incubation period and the time needed between the symptom onset and the infection detection/confirmation. We exploit this exponential regime to infer R_0 as described in Methods (see also (Magdalena Djordjevic et al., 2021) and (Salom et al., 2021)), which we further use as our independent (response) variable.

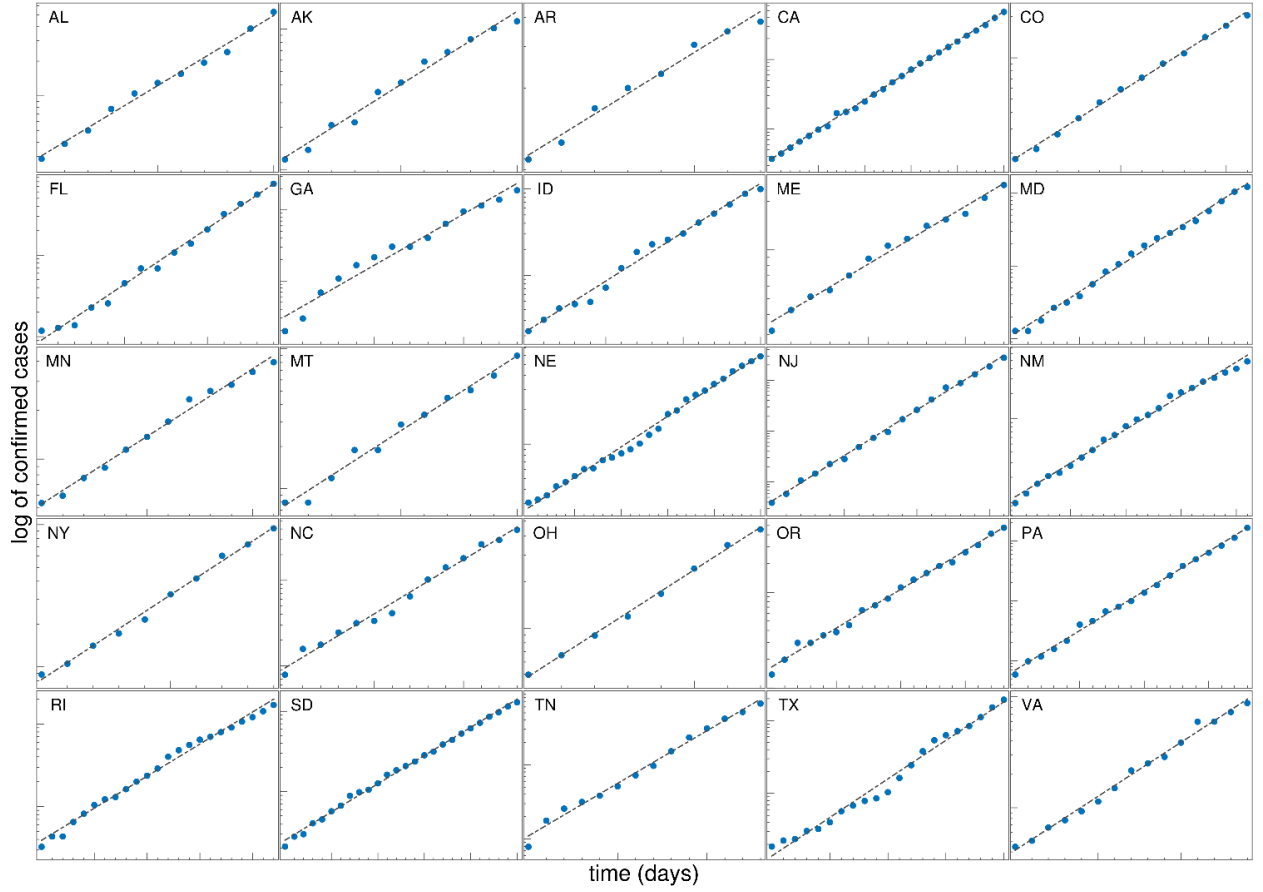


Figure 1. The time dependence of the detected cases for the different US states during the initial period of the epidemic is shown on a log-linear scale. The linear fit of $\log(D)$ shows that the spread of COVID-19 is well approximated by exponential growth in this phase. Values on axes are chosen differently for each state to emphasize the exponential growth phase. For each state, the start and end dates, the extracted slope λ_+ , of the exponential regime, are given in the Supplementary Table S1. AL – Alabama; AK – Arkansas; AR – Arizona; CA – California; CO – Colorado; FL – Florida; GA – Georgia; ID – Idaho; ME – Maine; MD – Maryland; MN – Montana; NE – Nebraska; NJ – New Jersey; NM – New Mexico; NY – New York; NC – North Carolina; OH – Ohio; OR – Oregon; PA – Pennsylvania; RI – Rhode Island; SD – South Dakota; TN – Tennessee; TX – Texas; VA – Virginia.

We further transformed the variables so that their distribution becomes as close to normal as possible and removed the outliers, as detailed in Methods. The main purpose of these transformations, and outliers' removal, is to account for more extreme variable values (such as heavy distribution tails), which may significantly affect some of the analysis methods that we further use (in particular, correlation analysis, Lasso and Elastic net regressions). On the other hand, methods based on the ensembles of decision trees (e.g., Random Forest and Gradient Boost) are fairly robust to outliers and non-normal variable distributions and will provide a consistency check of the obtained conclusions. Note that transformations of all variables are provided in Table 1. Further, the total number of variables (74) is larger than the sample size (46 states). While the regressions with feature selection (Lasso and Elastic net) can handle the number of variables that is significantly larger than the sample size (as long as the number of selected features is smaller than the sample size), this large number of variables (some highly correlated) is a major risk for overfitting, particularly for Random Forest and Gradient Boost methods.

To reduce both the number of variables and correlations between them, we employ PCA. The main disadvantage of this is possibly hard interpretation of the obtained PCs. We, thus, divided the initial set of variables into smaller subsets of similar meaning and high mutual correlation, where the division

of the variables into subgroups is provided in Table 2. Each group of variables is related to their corresponding PCs in that table. Note that the number of PCs for each variable group is chosen such that they explain more than 85% of the variability in the dataset (standard threshold). Finally, to each of the PCs, we assign an intuitive name (e.g., PC1 prosperity, PC1 age) according to the set of variables from which they are formed.

3.2 Feature extraction

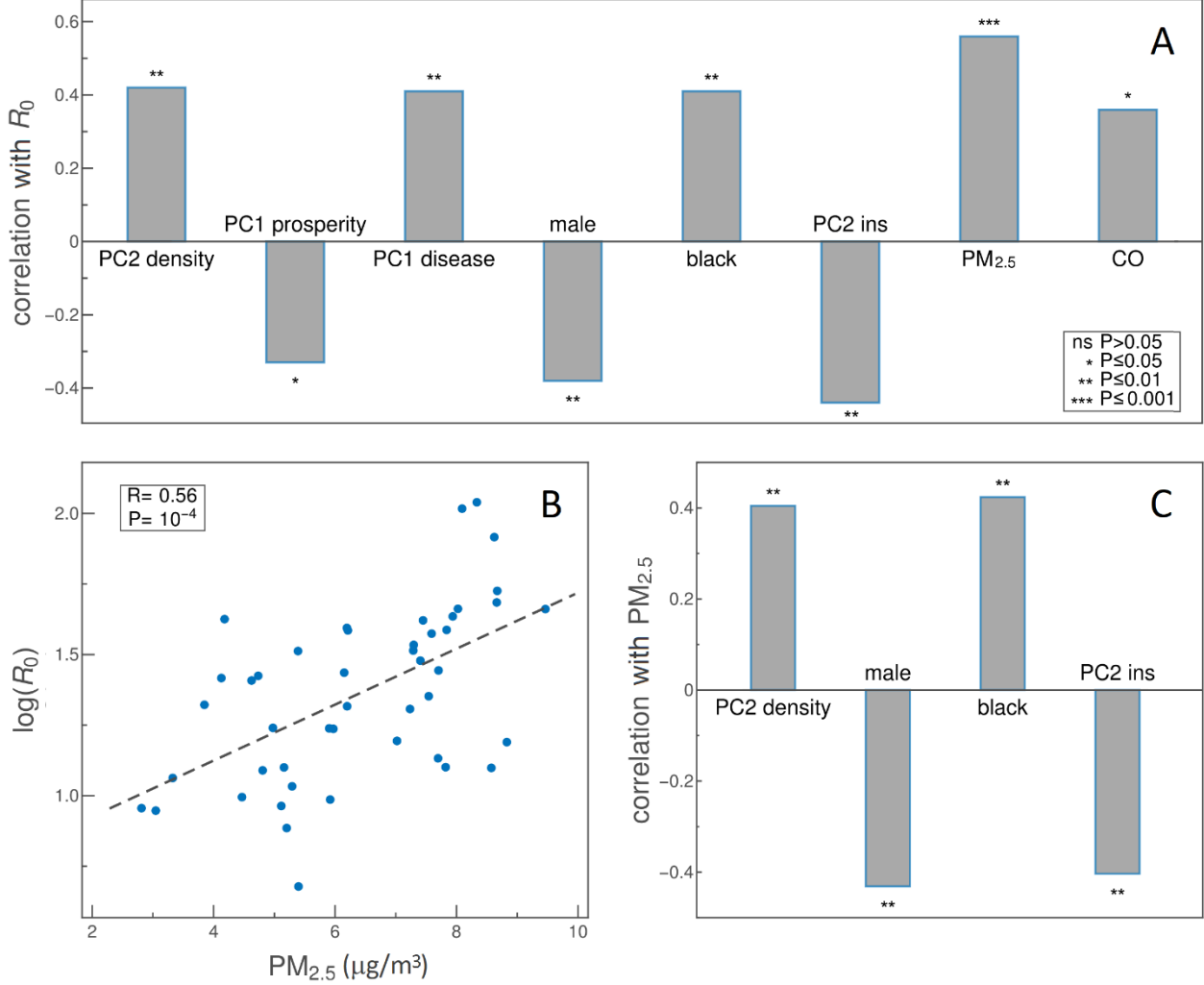


Figure 2. Pearson's correlations for relevant variables. A) Variables significantly correlated ($P < 0.05$) with the basic reproduction number R_0 are shown. The bars' height indicates the value of Pearson's correlation coefficient (R on the y axis). B) Scatter plot of R_0 vs. PM_{2.5}. The dashed line shows linear fit. C) Person's correlations of variables in A) with PM_{2.5}. Variable names are indicated on the horizontal axis. Stars in bar plots represent the level of statistical significance, as indicated in the figure legend.

We start from the basic assessment of the variable importance in explaining R_0 , which are pairwise correlations. Note that these do not control for the presence of other potentially important variables but are a straightforward initial assessment of the relation with R_0 . In Figure 2A, we show the Pearson correlation constant of the variables with R_0 , where predictors with statistically significant correlations ($P < 0.05$) are shown together with their correlation constants (represented by bars' heights) and statistical significance levels (indicated by stars). Somewhat surprisingly, we find that the highest correlation is with PM_{2.5}, with $R \sim 0.6$ and $P \sim 10^{-4}$. A large positive correlation between R_0 and PM_{2.5} levels can also be observed from the scatter plot in Figure 2B. Additionally, several other variables exhibit statistically significant correlations with R_0 , as indicated in Figure 2A. Note, however, that

some of these variables are also significantly correlated with $PM_{2.5}$. Moreover, their correlation with R_0 and $PM_{2.5}$ is in the same direction (Figure 2C). Consequently, their significant correlation with R_0 might, at least in part, be due to their correlation with $PM_{2.5}$.

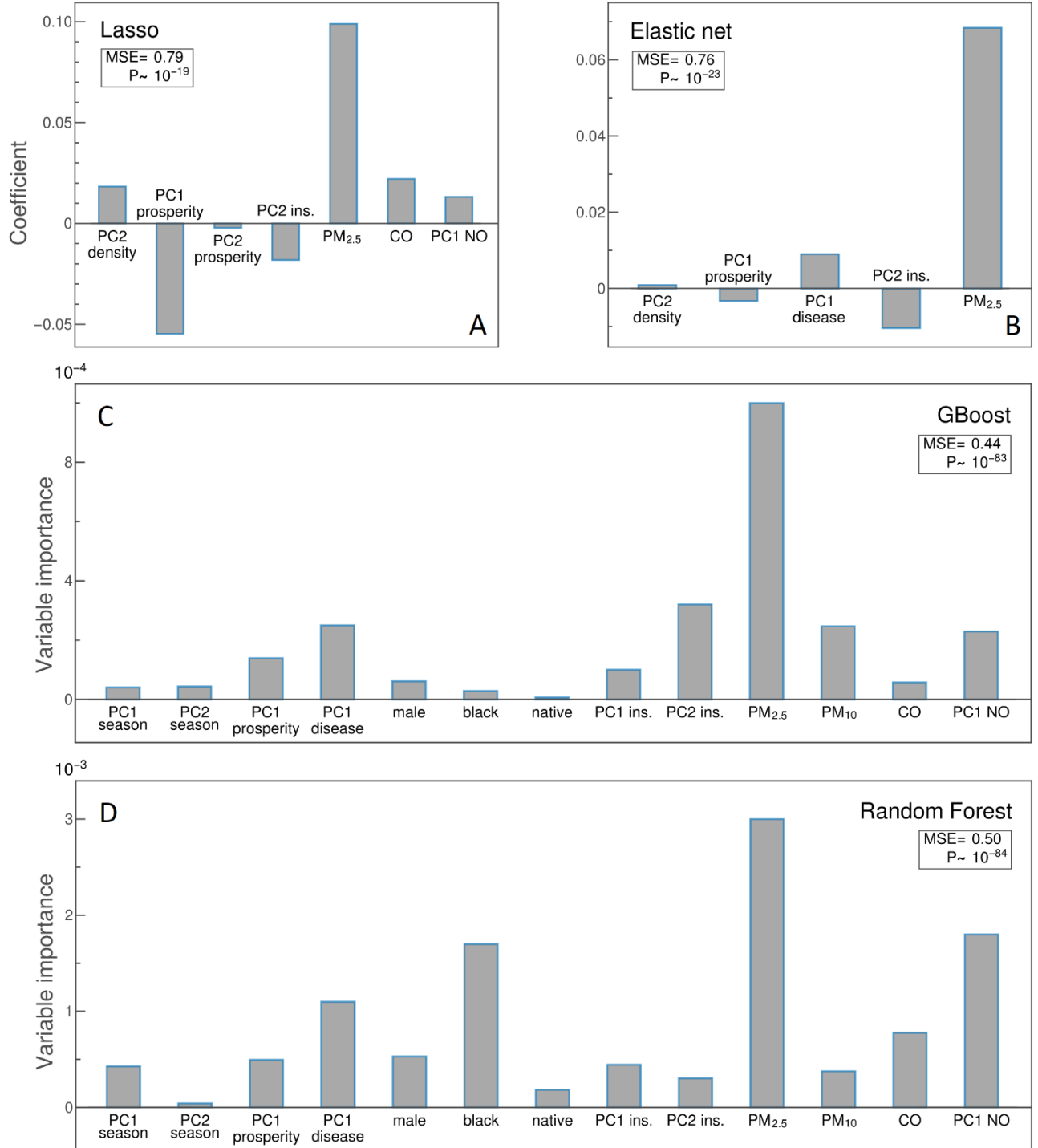


Figure 3: Values of regression coefficients in A) Lasso and B) Elastic Net regressions, respectively, where the bars' height corresponds to the coefficients' values for selected variables. Coefficients of all other variables are shrunk to zero (not shown) by the regressions. Variable importance in C) Gradient Boosting (GBoost) and D) Random Forest (RF) regressions, with the bars' height corresponding to estimated importance. Only variables with $P < 0.1$ (according to either Pearson, Kendall, or Spearman correlations with R_0) are included in GBoost and RF regressions. MSE values are scaled to the constant value model and averaged over 200 cross-validations. P -values correspond to the statistical significance of obtained MSE's compared to the baseline model. Variable names are indicated on the horizontal axis.

To partially address this, we proceed to an analysis that allows selecting the most important predictors from the set of correlated variables. Specifically, results of Lasso and Elastic net regressions are shown in Figures 3A and 3B. Both of these methods provide both regularization and the ability to select significant predictors through shrinking other coefficients to zero. Moreover, we standardize all the variables before using them in regressions, so that the absolute values of the regression coefficients provide relative importance of the selected variables. For each of the two methods, we perform repeated cross-validations, together with optimizations of hyperparameters, so that methods have maximal predictive power (i.e., minimal MSE) on the training set (see Methods for details). We obtain that the two methods are statistically highly significant compared to the constant model ($P \sim 10^{-19}$ and 10^{-23} , for Lasso and Elastic net, respectively). The predictive power of these methods is, however, only moderate, as can be seen for the obtained MSE values (MSEs are scaled, so that MSE of 1 corresponds to the constant model, which is not a large difference from 0.79 and 0.76, obtained by Lasso and Elastic net, respectively). Note, however, that the main purpose of these models is in feature selection, while predictability will be improved through models employed in the next subsection.

From both Lasso and Elastic net, we again obtain that $PM_{2.5}$ is the most important predictor, positively affecting COVID-19 transmissibility (so that higher $PM_{2.5}$ leads to higher transmissibility). A similar trend is obtained for CO and PC1 NO (formed from NO₂ and Nitrogen-oxides concentrations) – CO was also found to be significantly related with R_0 through pairwise correlations. Additionally, the population density (PC2 density) appears as an important predictor through both Lasso and Elastic net, though with smaller importance (regression coefficient), but consistently with pairwise correlations, and with a tendency to increase transmissibility. Also, through all three approaches employed so far (pairwise correlations, Lasso, and Elastic net), we obtain that the higher state prosperity (PC1 prosperity) negatively influences R_0 . Also, chronic diseases significantly influence (increase) R_0 as obtained by both pairwise correlations and Elastic net. Finally, PC2 ins., which is related to the fraction of the population (in particular Latinos) with medical insurance, also negatively correlates with R_0 (through all three methods). Interpretation of these dependencies is further addressed in the Discussion section.

3.3 Variable importance estimates

Our next goal is to assess variable importance and achieve better model predictability through methods that are considered state-of-the-art in machine learning for these types of problems. We will employ two methods based on ensembles of weak learners (decision trees), in particular Gradient Boost and Random Forest. They are substantially different from Lasso and Elastic net employed in the previous subsection, as they do not assume linear dependence of the response from input variables (so-called non-parametric models). Consequently, their employment provides an independent check for the importance of $PM_{2.5}$ in explaining R_0 . Moreover, we expect to obtain better predictability of these models, which can, in turn, be used for a quantitative estimate of pollution variation effects on R_0 .

The two methods are implemented similarly to Lasso and Elastic net, i.e., model hyperparameters are optimized to achieve maximal predictability through repeated cross-validations (see Method for details). As these models (i.e., decision trees in general) are prone to overfitting, we performed a simple variable selection. That is, only variables with $P < 0.1$ (according to either Pearson, Kendell, or Spearman correlations) are selected, resulting in 13 variables shown on the horizontal axes of Figures 3C and 3D, which were then used in further analysis. We obtained a much better predictive power for both Gradient Boost and Random Forest models (compared to regressions in the previous subsection) with MSE of 0.44 and 0.5, respectively, where these differences compared to the constant model (MSE=1) are statistically highly significant ($P \sim 10^{-83}$ and 10^{-84} , respectively).

Estimates of variable importance for both of these models are shown in Figures 3C and 3D. In both figures, the most prominent feature is $PM_{2.5}$, consistently with all other results obtained so far. Furthermore, PC1 disease and PC1 NO appear with moderate importance in both methods, where GBoost also emphasizes the importance of PC2 ins., which is all generally consistent with the analysis presented in the previous subsection. With respect to the pollution, the only difference is that PM_{10} appears as moderately important in GBoost, while not selected by other models. Also, CO is selected by Random Forest as moderately important (consistent with the previous analysis) but does not appear as such in GBoost. Finally, the racial factor (in particular, fraction of black population) is selected as important by Random Forest (and also appeared as significant through pairwise correlations) but does not appear as important in GBoost. A possible interpretation of these findings is addressed in the Discussion section.

3.4 Quantitative estimate of pollution influence on R_0

As we obtain a reasonable model accuracy through both GBoost and Random Forrest, we will next estimate how pollution variations (observed through different USA states) affect R_0 . While we included a substantial number of variables (all that we could realistically assemble) in our analysis, these are of course not all the variables that can affect R_0 , so we here aim to provide rough estimates. Still, such an estimate is useful, as it provides the magnitude by which reasonably realistic changes in the pollution levels can affect R_0 . For example, the new SARS-CoV-2 strain that emerged in Great Britain (known as B.1.1.7), which is considered to become dominant in many other parts of the world, is estimated to lead to up to 1.9 increase in R_0 – this value can e.g. be compared with our estimated change due to pollution variations. To generate predictions for each of the analyzed states, we keep all other parameters fixed while changing the pollution values so that the changes correspond to the actual values observed in all 46 states. In this way, the relative change in R_0 , due to observed variations in pollution ($\Delta R_0/R_0$) was estimated, where ΔR_0 corresponds to the difference between maximal and minimal estimated R_0 values.

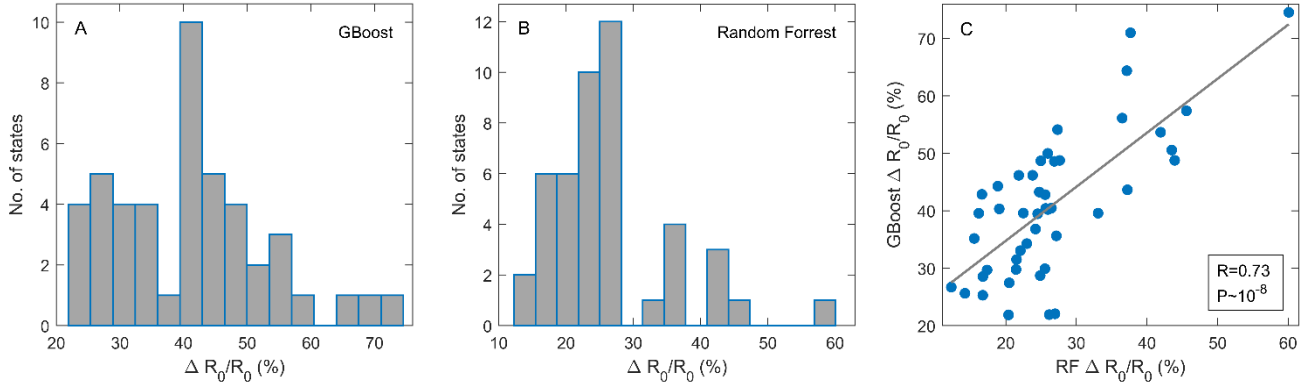


Figure 4: Relative change in R_0 due to pollution variations observed in USA states. For each state included in the analysis, R_0 was predicted for the range of pollution values observed throughout all other states. Relative variation in R_0 was estimated through both A) Gradient Boost (GBoost) and B) Random Forest (RF) regressions, with the models trained as in Fig. 3C) Scatter plot of $\Delta R_0/R_0$ predictions for GBoost and RF, with Pearson’s correlation coefficient and P -value indicated.

The obtained results for $\Delta R_0/R_0$ for all analyzed states are shown as histograms in Figure 4A (GBoost) and 4B (Random Forest). For GBoost, a somewhat larger $\Delta R_0/R_0$, corresponding to the median of $\sim 40\%$, is obtained, while for Random Forrest, smaller values with a median of $\sim 25\%$ are estimated. This can e.g. be compared with $\Delta R_0/R_0$ of up to 90% for the B.1.1.7 strain (Davies et al., 2021), so that estimated changes due to pollution variation are smaller but still substantial. Finally, as the two

histograms are somewhat different, in Figure 4C we directly test the consistency of their $\Delta R_0/R_0$ predictions. It can be seen that they are well consistent, with reasonably high correlation ($R=0.73$ and $P\sim 10^{-8}$). Note that these two methods are independent and substantially different (though both based on ensembles of decision trees), so differences in their predictions are expected.

4 Discussion

Figures 2 and 3 reveal the main paper conclusion: $PM_{2.5}$ pollution is the main driver behind SARS-CoV-2 transmissibility in the US. This result is unambiguously obtained through both pairwise correlations of variables with R_0 and by the applied machine learning approaches. While the association of the $PM_{2.5}$ pollution with the rate of COVID19 spread is not a novel result (Gujral and Sinha, 2021; Gupta and Gharehgozli, 2020; Maleki et al., 2021; Stieb et al., 2020), this research is distinct from the existing studies: First, through its large robustness, where we reached the same conclusion by diverse approaches, as illustrated in Figure 3. Secondly, by explicitly taking into account the infection dynamics, i.e., the model-based estimate of R_0 as SARS-CoV-2 transmissibility measure, ensuring that the result does not depend on testing and/or the implemented social distancing measures. This study is also distinct due to the sheer number of 74 predictors initially considered, where PCA and different statistical learning approaches were used to analyze such a large feature set in a meaningful way that allows straightforward interpretation. Taken together, we believe that the results presented here establish the link of $PM_{2.5}$ pollution with COVID19 transmissibility much more firmly. Previous studies on the USA obtained non-consistent reports on pollution importance, underlying importance of more extensive modeling and statistical learning approaches that we employed here (Allen et al., 2021; Gupta and Gharehgozli, 2020; Luo et al., 2021).

A quantitative implication of the established connection is illustrated in Figure 4. We estimated that varying the pollutant levels (specifically, levels of $PM_{2.5}$, PM_{10} , CO and NO_2 , which enter Random Forest and Gradient Boost methods), where changes in $PM_{2.5}$ levels are by far the most important, they make a difference of $\sim 30\%$ in terms of the R_0 values. While this is smaller compared to reproduction number changes due to the appearance of new highly infective strains (that are up to $\sim 90\%$ higher) (Davies et al., 2021), it is still sizable, and clearly illustrates the importance of $PM_{2.5}$ in modulating the virus transmissibility. For example, in an exponential regime of infection progression (c.f. Eq. (3.8) in Methods) lasting for ~ 10 days (a typical period in which exponential growth is observed for USA states), and with typical parameter values, leads to two times larger number of infected, and (at least) equal proportion of lost human lives. An additional (and independent) effect of larger pollutant levels, is in potentially increased COVID-19 mortality due to higher pollutant levels, as suggested by several studies (Luo et al., 2021; Pozzer et al., 2020; X. Wu et al., 2020). Overall, this underscores the importance of reducing pollutant levels in the epidemiological context.

While we obtain that $PM_{2.5}$ pollution is the dominant predictor of virus transmissibility, our results also suggest the relevance of other factors. First, few other pollutants are also selected through our analysis, most notably NO_2 and its related nitrogen oxide derivatives (where its particularly high importance was assigned by the Random Forest method, see Fig. 3D), and to some extent CO and PM_{10} . These results are partially in line with findings that a number of pollutants, more precisely particulate matter (Comunian et al., 2020; Sagawa et al., 2021), but also NO_2 (Paital and Agrawal, 2020), cause overexpression of ACE-2 in respiratory cells, thus increasing the likelihood of infection. This is not necessarily the only relevant mechanism, as the prolonged exposure to pollutants can cause a general weakening of the immune system (Glencross et al., 2020; Qu et al., 2020). However, the relatively low importance of NO and CO pollutants that we obtained speaks in favor of the hypothesis that PM pollution, by binding to virus droplets, additionally mechanically facilitates SARS-CoV-2 spread through the air - both extending the range of virus diffusion and allowing its direct transport into deeper

pulmonary regions (Qu et al., 2020). On the other hand, the inferred large difference in the influence of $PM_{2.5}$ and PM_{10} particles may be understood through the difficulty of particulate matter larger than $5\text{ }\mu\text{m}$ to reach ACE2 receptors located in type II alveolar cells (Bontempi, 2020; Copat et al., 2020; Zhu et al., 2020).

Another factor (unsurprisingly) related to the susceptibility of an organism to infections, is the presence of different comorbidities and, in general, any diseases that could potentially compromise the immune system (Allel et al., 2020; Coccia, 2020; Liu et al., 2020). Indeed, all applied analysis methods except for Lasso, find the prevalence of chronic diseases in the population (i.e., its dominant principal component PC1-disease) to be an important R_0 predictor.

Additionally, the applied methods also identify a group of three mutually interrelated factors: the dominant PC reflecting the overall prosperity of the state (PC1 prosperity), the percentage of the black population, and the PC2 insurance component (this component effectively reflects the insurance coverage among the Hispanic population). Our recent study of the effects of various demographic and weather parameters on the spread of COVID19 based on the data from 118 world countries (Marko Djordjevic et al., 2021) also pointed to the essential role of the country's prosperity, but we note a stark disagreement in the sign of the correlation: whereas, worldwide, the more developed countries suffered from higher COVID19 expansion rates, data on US states show an opposite trend - wealthier and more developed areas of US on average seem to exhibit lower R_0 values (Gupta and Gharehgozli, 2020). However, this difference may be expected: on the global level, there are substantial variations in the development level between countries, where this level effectively becomes a proxy for the frequency of social contacts (reflecting business and cultural activity, population mixing due to work/education, international travel, etc.) (Gangemi et al., 2020). On the other hand, all states of America have highly developed societies and the dominant effect of these more subtle differences is likely different: within this prosperity range, the better off population has more means to prioritize and practice precautionary behavior (e.g. have professions that require less physical contacts, fewer comorbidities, healthier lifestyle, higher awareness of the infection risks, etc.). But a COVID19 pandemic has also emphasized a specific racial aspect of healthcare disparities. The correlation between the percentage of the black population and R_0 observed in our data (Figure 2A), as well as the results of the Random Forrest regression method (Figure 3D), agree with the already established conclusion that the black minority is by far overrepresented not only among COVID19 fatalities (Luo et al., 2021; Xiao Wu et al., 2020) but also among the total infected population (Chakraborty, 2021; Stieb et al., 2020). Another relevant factor is the health insurance coverage (PC2 insurance), which consistently through our analysis shows that COVID19 infection is spreading faster among people without medical insurance (Figure 2 and Figure 3). Both the percentage of the black population and the prevalence of insurance coverage are significantly correlated with pollution, in particular with $PM_{2.5}$, as can be seen in Figure 2C (curiously, our data do not show such correlation with the PC1 prosperity component). It has been argued that the influence of factors related to a more economically disadvantaged population (overrepresentation of minorities, absence of medical insurance,...) is inherently hard to disentangle from the effects of pollution. While this standpoint is also in part supported by our analysis, we also note that $PM_{2.5}$ consistently appeared with much larger importance through all analyses compared to these economically disadvantaged factors (Chakraborty, 2021; Stieb et al., 2020). Therefore, the most plausible interpretation is to associate $PM_{2.5}$ (rather than these other factors) with R_0 changes.

It is also interesting to consider which parameters did not show up as important in our results. The absence of seasonal principal components from the final sets of significant predictors may imply irrelevance of the weather parameters such as temperature, UV radiation, and humidity on the SARS-CoV2 transmission - in spite that it has become almost a common knowledge that high temperatures should suppress the virus transmission (Byun et al., 2021; Fu et al., 2021; Sarkodie and Owusu, 2020).

Thus, the results presented here side with the authors who disagree that weather factors bear a significant influence on the course of the COVID19 epidemic (Wang et al., 2021). One should however note that variations of meteorological factors are much larger on a global scale, where indeed we find out a larger significance of these factors (Salom et al., 2021). Another somewhat surprising conclusion is the moderate significance of the population density. While there is a significant correlation of PC2 density component with R_0 , it further appeared significant only in Lasso regression, and even there with not that high coefficient. This is however in line with several other studies, that also didn't assign a high significance to population density (Carozzi et al., 2020; Hamidi et al., 2020; Pourghasemi et al., 2020; Rashed et al., 2020).

5 Conclusion and outlook

Starting from 74 initial parameters and by using five different analysis approaches, we obtained the results that robustly select $PM_{2.5}$ pollution as the most important predictor of SARS-CoV-2 transmissibility in the USA. Using R_0 as a transmissibility measure and non-linear dynamics to extract its values for different USA states, these results are largely insensitive to the differences in the state policies. The obtained large quantitative estimate of the magnitude of the $PM_{2.5}$ effect on virus transmissibility may be intuitively unexpected and is not that far from estimated differences in transmissibility caused by virus mutations.

The main issue to be addressed in future studies is that of causality, i.e. disentangling the effects of pollution from those of socio-demographic factors with which it is correlated. This clearly cannot be achieved through studies with a larger resolution, such as the one employed here, even with applications of sophisticated statistical (machine) learning methods, and with taking into account the infection progression dynamics. Carefully crafted, and high resolution, longitudinal epidemiological studies may be a way forward in this regard. The results obtained here, and by other similar studies, may provide a basis for these high-resolution studies, particularly in terms of factors that should be considered, their expected relative importance, and the magnitude of the effects that may be expected.

6 Conflict of Interest

The authors declare that the research was conducted in the absence of any commercial or financial relationships that could be construed as a potential conflict of interest.

7 Author Contributions

MarD, IS and MagD conceived the research. The work was supervised by MarD, IS and AR. Data acquisition and supplementary material by OM, MT and DZ. Code writing and data analysis by OM, MarD, DZ, SM. Figures and tables made by OM, DZ, MT and MagD. Literature search by AR and SM. Result interpretation by MarD, MagD, IS, AR and SM. Manuscript written by MarD, IS, AR, MagD, OM and MT.

8 Data Availability Statement

Data is provided in provided in the Supplementary material.

9 Funding

This work was partially supported by the Ministry of Education, Science and Technological Development of the Republic of Serbia.

10 References

- Adhikari, A., Yin, J., 2020. Short-Term Effects of Ambient Ozone, PM(2.5,) and Meteorological Factors on COVID-19 Confirmed Cases and Deaths in Queens, New York. *Int J Environ Res Public Health* 17, 4047. <https://doi.org/10.3390/ijerph17114047>
- Allel, K., Tapia-Muñoz, T., Morris, W., 2020. Country-level factors associated with the early spread of COVID-19 cases at 5, 10 and 15 days since the onset. *medRxiv* 15, 1589–1602. <https://doi.org/10.1080/17441692.2020.1814835>
- Allen, O., Brown, A., Wang, E., 2021. Socioeconomic Disparities in the Effects of Pollution on Spread of Covid-19: Evidence from US Counties. *medRxiv*. <https://doi.org/10.1101/2021.01.06.21249303>
- America's Health Ranking, 2021. America's Health Rankings analysis of CDC, Behavioral Risk Factor Surveillance System, United Health Foundation. America's Health Rankings. URL <https://www.americashealthrankings.org/> (accessed 3.28.21).
- Bontempi, E., 2020. First data analysis about possible COVID-19 virus airborne diffusion due to air particulate matter (PM): The case of Lombardy (Italy). *Environmental Research* 186, 109639. <https://doi.org/10.1016/j.envres.2020.109639>
- Breiman, L., 2001. Random Forests. *Machine Learning* 45, 5–32. <https://doi.org/10.1023/A:1010933404324>
- Breiman, L., 1996. Bagging predictors. *Machine Learning* 24, 123–140. <https://doi.org/10.1007/BF00058655>
- Byun, W.S., Heo, S.W., Jo, G., Kim, J.W., Kim, S., Lee, S., Park, H.E., Baek, J.-H., 2021. Is coronavirus disease (COVID-19) seasonal? A critical analysis of empirical and epidemiological studies at global and local scales. *Environmental Research* 196, 110972. <https://doi.org/10.1016/j.envres.2021.110972>
- Carozzi, F., Provenzano, S., Roth, S., 2020. Urban Density and COVID-19 (IZA Discussion Paper No. 13440). Institute of Labor Economics (IZA), Bonn.
- CDC, 2019. CDC - Behavioral Risk Factor Surveillance System. URL <https://www.cdc.gov/brfss/index.html> (accessed 3.28.21).
- Chakraborty, J., 2021. Convergence of COVID-19 and chronic air pollution risks: Racial/ethnic and socioeconomic inequities in the U.S. *Environmental Research* 193, 110586. <https://doi.org/10.1016/j.envres.2020.110586>
- Chen, P.-S., Tsai, F.T., Lin, C.K., Yang, C.-Y., Chan, C.-C., Young, C.-Y., Lee, C.-H., 2010. Ambient influenza and avian influenza virus during dust storm days and background days. *Environ Health Perspect* 118, 1211–1216. <https://doi.org/10.1289/ehp.0901782>
- Coccia, M., 2020. An index to quantify environmental risk of exposure to future epidemics of the COVID-19 and similar viral agents: Theory and practice. *Environ Res* 191, 110155–110155. <https://doi.org/10.1016/j.envres.2020.110155>
- Comunian, S., Dongo, D., Milani, C., Palestini, P., 2020. Air Pollution and Covid-19: The Role of Particulate Matter in the Spread and Increase of Covid-19's Morbidity and Mortality. *Int J Environ Res Public Health* 17, 4487. <https://doi.org/10.3390/ijerph17124487>
- Contini, D., Costabile, F., 2020. Does Air Pollution Influence COVID-19 Outbreaks? *Atmosphere* 11. <https://doi.org/10.3390/atmos11040377>
- Copat, C., Cristaldi, A., Fiore, M., Grasso, A., Zuccarello, P., Signorelli, S.S., Conti, G.O., Ferrante, M., 2020. The role of air pollution (PM and NO₂) in COVID-19 spread and lethality: A systematic review. *Environmental Research* 191, 110129. <https://doi.org/10.1016/j.envres.2020.110129>
- Davies, N.G., Abbott, S., Barnard, R.C., Jarvis, C.I., Kucharski, A.J., Munday, J.D., Pearson, C.A.B., Russell, T.W., Tully, D.C., Washburne, A.D., Wenseleers, T., Gimma, A., Waites, W., Wong,

- K.L.M., van Zandvoort, K., Silverman, J.D., Diaz-Ordaz, K., Keogh, R., Eggo, R.M., Funk, S., Jit, M., Atkins, K.E., Edmunds, W.J., 2021. Estimated transmissibility and impact of SARS-CoV-2 lineage B.1.1.7 in England. *Science* 372. <https://doi.org/10.1126/science.abg3055>
- De Angelis, E., Renzetti, S., Volta, M., Donato, F., Calza, S., Placidi, D., Lucchini, R.G., Rota, M., 2021. COVID-19 incidence and mortality in Lombardy, Italy: An ecological study on the role of air pollution, meteorological factors, demographic and socioeconomic variables. *Environmental Research* 195, 110777. <https://doi.org/10.1016/j.envres.2021.110777>
- Djordjevic, Magdalena, Djordjevic, Marko, Ilic, B., Stojku, S., Salom, I., 2021. Understanding Infection Progression under Strong Control Measures through Universal COVID-19 Growth Signatures. *Global Challenges* 2000101. <https://doi.org/10.1002/gch2.202000101>
- Djordjevic, Marko, Salom, I., Markovic, S., Rodic, A., Milicevic, O., Djordjevic, Magdalena, 2021. Inferring the main drivers of SARS-CoV-2 transmissibility, *arXiv:2103.15123*.
- Domingo, J.L., Rovira, J., 2020. Effects of air pollutants on the transmission and severity of respiratory viral infections. *Environmental Research* 187, 109650. <https://doi.org/10.1016/j.envres.2020.109650>
- Freund, Y., Schapire, R.E., 1997. A Decision-Theoretic Generalization of On-Line Learning and an Application to Boosting. *Journal of Computer and System Sciences* 55, 119–139. <https://doi.org/10.1006/jcss.1997.1504>
- Friedman, J.H., 2001. Greedy Function Approximation: A Gradient Boosting Machine. *The Annals of Statistics* 29, 1189–1232.
- Friedman, J.H., Hastie, T., Tibshirani, R., 2010. Regularization Paths for Generalized Linear Models via Coordinate Descent. *Journal of Statistical Software, Articles* 33, 1–22. <https://doi.org/10.18637/jss.v033.i01>
- Fu, S., Wang, B., Zhou, J., Xu, X., Liu, J., Ma, Y., Li, L., He, X., Li, S., Niu, J., Luo, B., Zhang, K., 2021. Meteorological factors, governmental responses and COVID-19: Evidence from four European countries. *Environmental Research* 194, 110596. <https://doi.org/10.1016/j.envres.2020.110596>
- Gangemi, S., Billeci, L., Tonacci, A., 2020. Rich at risk: socio-economic drivers of COVID-19 pandemic spread. *Clinical and Molecular Allergy* 18, 12. <https://doi.org/10.1186/s12948-020-00127-4>
- Glencross, D.A., Ho, T.-R., Camiña, N., Hawrylowicz, C.M., Pfeffer, P.E., 2020. Air pollution and its effects on the immune system. *Free Radical Biology and Medicine* 151, 56–68. <https://doi.org/10.1016/j.freeradbiomed.2020.01.179>
- Gujral, H., Sinha, A., 2021. Association between exposure to airborne pollutants and COVID-19 in Los Angeles, United States with ensemble-based dynamic emission model. *Environmental Research* 194, 110704. <https://doi.org/10.1016/j.envres.2020.110704>
- Gupta, A., Gharehgozli, A., 2020. Developing a Machine Learning Framework to Determine the Spread of COVID-19. <http://dx.doi.org/10.2139/ssrn.3635211>
- Hamidi, S., Sabouri, S., Ewing, R., 2020. Does Density Aggravate the COVID-19 Pandemic? *null* 86, 495–509. <https://doi.org/10.1080/01944363.2020.1777891>
- Hastie, T., Tibshirani, R., Friedman, J., 2008. *The Elements of Statistical Learning*, 2nd edition. ed. Springer, New York.
- Keeling, M.J., Rohani, P., 2011. *Modeling Infectious Diseases in Humans and Animals*. Princeton University Press, Princeton, NJ.
- Krstajic, D., Buturovic, L.J., Leahy, D.E., Thomas, S., 2014. Cross-validation pitfalls when selecting and assessing regression and classification models. *J Cheminform* 6, 10–10. <https://doi.org/10.1186/1758-2946-6-10>

- Liu, H., Chen, S., Liu, M., Nie, H., Lu, H., 2020. Comorbid Chronic Diseases are Strongly Correlated with Disease Severity among COVID-19 Patients: A Systematic Review and Meta-Analysis. *Aging Dis* 11, 668–678. <https://doi.org/10.14336/AD.2020.0502>
- Lorenzo, J.S.L., Tam, W.W.S., Seow, W.J., 2021. Association between air quality, meteorological factors and COVID-19 infection case numbers. *Environmental Research* 197, 111024. <https://doi.org/10.1016/j.envres.2021.111024>
- Luo, Y., Yan, J., McClure, S., 2021. Distribution of the environmental and socioeconomic risk factors on COVID-19 death rate across continental USA: a spatial nonlinear analysis. *Environ Sci Pollut Res Int* 28, 6587–6599. <https://doi.org/10.1007/s11356-020-10962-2>
- Maier, B.F., Brockmann, D., 2020. Effective containment explains subexponential growth in recent confirmed COVID-19 cases in China. *Science* 368, 742–746. <https://doi.org/10.1126/science.abb4557>
- Maleki, M., Anvari, E., Hopke, P.K., Noorimotlagh, Z., Mirzaee, S.A., 2021. An updated systematic review on the association between atmospheric particulate matter pollution and prevalence of SARS-CoV-2. *Environmental Research* 195, 110898. <https://doi.org/10.1016/j.envres.2021.110898>
- Martcheva, M., 2015. *An Introduction to Mathematical Epidemiology*. Springer, Boston, MA.
- Maslov, S., Goldenfeld, N., 2020. Window of Opportunity for Mitigation to Prevent Overflow of ICU capacity in Chicago by COVID-19. <https://doi.org/10.1101/2020.03.20.20040048>
- Measure of America, 2018. Mapping America: Demographic Indicators. URL <http://measureofamerica.org/tools-old/> (accessed 3.28.21).
- NASA Langley Research Center, 2020. The Prediction of Worldwide Energy Resources (POWER) Project. URL <https://power.larc.nasa.gov/> (accessed 3.28.21).
- OpenUV, 2020. Global UV Index API. OpenUV. URL <https://www.openuv.io/> (accessed 3.28.21).
- Paital, B., Agrawal, P.K., 2020. Air pollution by NO₂ and PM_{2.5} explains COVID-19 infection severity by overexpression of angiotensin-converting enzyme 2 in respiratory cells: a review. *Environ Chem Lett* 1–18. <https://doi.org/10.1007/s10311-020-01091-w>
- Perkins, T.A., España, G., 2020. Optimal Control of the COVID-19 Pandemic with Non-pharmaceutical Interventions. *Bulletin of Mathematical Biology* 82, 118. <https://doi.org/10.1007/s11538-020-00795-y>
- Pourghasemi, H.R., Pouyan, S., Heidari, B., Farajzadeh, Z., Fallah Shamsi, S.R., Babaei, S., Khosravi, R., Etemadi, M., Ghanbarian, G., Farhadi, A., Safaeian, R., Heidari, Z., Tarazkar, M.H., Tiefenbacher, J.P., Azmi, A., Sadeghian, F., 2020. Spatial modeling, risk mapping, change detection, and outbreak trend analysis of coronavirus (COVID-19) in Iran (days between February 19 and June 14, 2020). *International Journal of Infectious Diseases* 98. <https://doi.org/10.1016/j.ijid.2020.06.058>
- Pozzer, A., Dominici, F., Haines, A., Witt, C., Münzel, T., Lelieveld, J., 2020. Regional and global contributions of air pollution to risk of death from COVID-19. *Cardiovascular Research* 116, 2247–2253. <https://doi.org/10.1093/cvr/cvaa288>
- Qu, G., Li, X., Hu, L., Jiang, G., 2020. An Imperative Need for Research on the Role of Environmental Factors in Transmission of Novel Coronavirus (COVID-19). *Environ Sci Technol* 54, 3730–3732. <https://doi.org/10.1021/acs.est.0c01102>
- Rashed, E.A., Koder, S., Gomez-Tames, J., Hirata, A., 2020. Influence of Absolute Humidity, Temperature and Population Density on COVID-19 Spread and Decay Durations: Multi-Prefecture Study in Japan. *International Journal of Environmental Research and Public Health* 17. <https://doi.org/10.3390/ijerph17155354>
- Sagawa, T., Tsujikawa, T., Honda, A., Miyasaka, N., Tanaka, M., Kida, T., Hasegawa, K., Okuda, T., Kawahito, Y., Takano, H., 2021. Exposure to particulate matter upregulates ACE2 and

- TMPRSS2 expression in the murine lung. *Environmental Research* 195, 110722. <https://doi.org/10.1016/j.envres.2021.110722>
- Salom, I., Rodic, A., Milicevic, O., Zigic, D., Djordjevic, Magdalena, Djordjevic, Marko, 2021. Effects of Demographic and Weather Parameters on COVID-19 Basic Reproduction Number. *Frontiers in Ecology and Evolution* 8, 524. <https://doi.org/10.3389/fevo.2020.617841>
- Sarkodie, S.A., Owusu, P.A., 2020. Impact of meteorological factors on COVID-19 pandemic: Evidence from top 20 countries with confirmed cases. *Environmental Research* 191, 110101. <https://doi.org/10.1016/j.envres.2020.110101>
- Smits, J., Permanyer, I., 2019. The Subnational Human Development Database. *Scientific Data* 6, 190038. <https://doi.org/10.1038/sdata.2019.38>
- Stieb, D.M., Evans, G.J., To, T.M., Brook, J.R., Burnett, R.T., 2020. An ecological analysis of long-term exposure to PM_{2.5} and incidence of COVID-19 in Canadian health regions. *Environmental Research* 191, 110052. <https://doi.org/10.1016/j.envres.2020.110052>
- Suhaimi, N.F., Jalaludin, J., Latif, M.T., 2020. Demystifying a Possible Relationship between COVID-19, Air Quality and Meteorological Factors: Evidence from Kuala Lumpur, Malaysia. *Aerosol and Air Quality Research* 20, 1520–1529. <https://doi.org/10.4209/aaqr.2020.05.0218>
- Tello-Leal, E., Macías-Hernández, B.A., 2020. Association of environmental and meteorological factors on the spread of COVID-19 in Victoria, Mexico, and air quality during the lockdown. *Environmental Research* 110442. <https://doi.org/10.1016/j.envres.2020.110442>
- Tian, H., Liu, Y., Li, Y., Wu, C.-H., Chen, B., Kraemer, M.U.G., Li, B., Cai, J., Xu, B., Yang, Q., Wang, B., Yang, P., Cui, Y., Song, Y., Zheng, P., Wang, Q., Bjornstad, O.N., Yang, R., Grenfell, B.T., Pybus, O.G., Dye, C., 2020. An investigation of transmission control measures during the first 50 days of the COVID-19 epidemic in China. *Science* 368, 638–642. <https://doi.org/10.1126/science.abb6105>
- Tibshirani, R., 1996. Regression Shrinkage and Selection Via the Lasso. *Journal of the Royal Statistical Society: Series B (Methodological)* 58, 267–288. <https://doi.org/10.1111/j.2517-6161.1996.tb02080.x>
- U.S. Census Bureau, 2020. U.S. Census. URL <https://www.census.gov/en.html> (accessed 3.28.21).
- U.S. Census Bureau, 2019. Nativity in the United States American Community Survey 1-year estimates. URL <https://censusreporter.org/> (accessed 3.28.21).
- U.S. Census Bureau, Population Division, 2019. Annual Estimates of the Resident Population by Single Year of Age and Sex for the United States, States, and Puerto Rico Commonwealth: April 1, 2010, to July 1, 2018. URL <https://www.census.gov/en.html> (accessed 3.28.21).
- US Environmental Protection Agency, 2020. Air Quality System Data. US EPA. URL <https://www.epa.gov/outdoor-air-quality-data> (accessed 3.28.21).
- Wang, Q., Zhao, Yu, Zhang, Yajuan, Qiu, J., Li, J., Yan, N., Li, N., Zhang, J., Tian, D., Sha, X., Jing, J., Yang, C., Wang, K., Xu, R., Zhang, Yuhong, Yang, H., Zhao, S., Zhao, Yi, 2021. Could the ambient higher temperature decrease the transmissibility of COVID-19 in China? *Environmental Research* 193, 110576. <https://doi.org/10.1016/j.envres.2020.110576>
- Weitz, J.S., Beckett, S.J., Coenen, A.R., Demory, D., Dominguez-Mirazo, M., Dushoff, J., Leung, C.-Y., Li, G., Măgălie, A., Park, S.W., Rodriguez-Gonzalez, R., Shivam, S., Zhao, C.Y., 2020. Modeling shield immunity to reduce COVID-19 epidemic spread. *Nature Medicine* 26, 849–854. <https://doi.org/10.1038/s41591-020-0895-3>
- Wikipedia, 2021a. List of states and territories of the United States by population. URL https://en.wikipedia.org/w/index.php?title=List_of_states_and_territories_of_the_United_States_by_population&oldid=1016990633 (accessed 3.28.21).
- Wikipedia, 2021b. List of United States cities by population. URL https://en.wikipedia.org/w/index.php?title=List_of_United_States_cities_by_population&oldid=1017904123 (accessed 3.28.21).

- Wu, X., Nethery, R.C., Sabath, M.B., Braun, D., Dominici, F., 2020. Air pollution and COVID-19 mortality in the United States: Strengths and limitations of an ecological regression analysis. *Science Advances* 6. <https://doi.org/10.1126/sciadv.abd4049>
- Wu, Xiao, Nethery, R.C., Sabath, M.B., Braun, D., Dominici, F., 2020. Exposure to air pollution and COVID-19 mortality in the United States: A nationwide cross-sectional study. *medRxiv* 2020.04.05.20054502. <https://doi.org/10.1101/2020.04.05.20054502>
- Yao, Y., Pan, J., Liu, Z., Meng, X., Wang, Weidong, Kan, H., Wang, Weibing, 2021. Ambient nitrogen dioxide pollution and spreadability of COVID-19 in Chinese cities. *Ecotoxicology and Environmental Safety* 208, 111421. <https://doi.org/10.1016/j.ecoenv.2020.111421>
- Zhu, Y., Xie, J., Huang, F., Cao, L., 2020. Association between short-term exposure to air pollution and COVID-19 infection: Evidence from China. *Science of The Total Environment* 727, 138704. <https://doi.org/10.1016/j.scitotenv.2020.138704>
- Zou, H., Hastie, T., 2005. Regularization and Variable Selection via the Elastic Net. *Journal of the Royal Statistical Society. Series B (Statistical Methodology)* 67, 301–320.
- Worldometer, 2020. COVID-19 Coronavirus Pandemic [Online]. Available online at: <https://www.worldometers.info/coronavirus/> (accessed January 14, 2021).